Supplementary Information

Manuscript: *Fibroblast-enriched senescence-associated transcription and measurement-context-dependent FAP–matrix covariation in colorectal cancer*

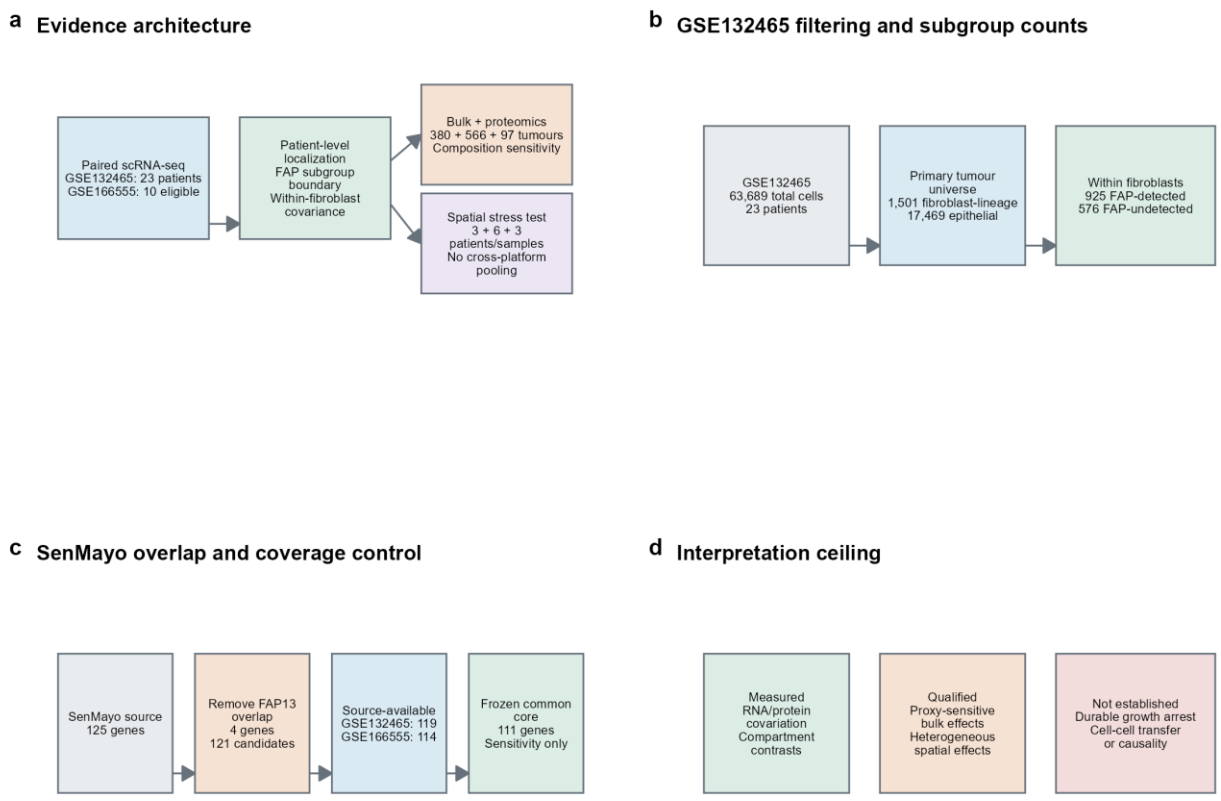
Overview

The Supplementary Information comprises seven figures, eight tables, four companion source-data files and a CAF source-data archive. The inferential unit is the patient or independent tumour sample wherever biological replication is available. Cell, bin and spot counts describe measurement density and are not treated as independent biological replicates. SenMayo and SASP scores localize senescence-associated transcription; they do not diagnose durable cellular senescence. FAP-detected denotes RNA detection and does not imply protein positivity.

The 111-gene SenMayo common core is a cross-dataset sensitivity definition. Source-available SenMayo definitions remain primary within each cohort, and effects are not pooled across platforms.

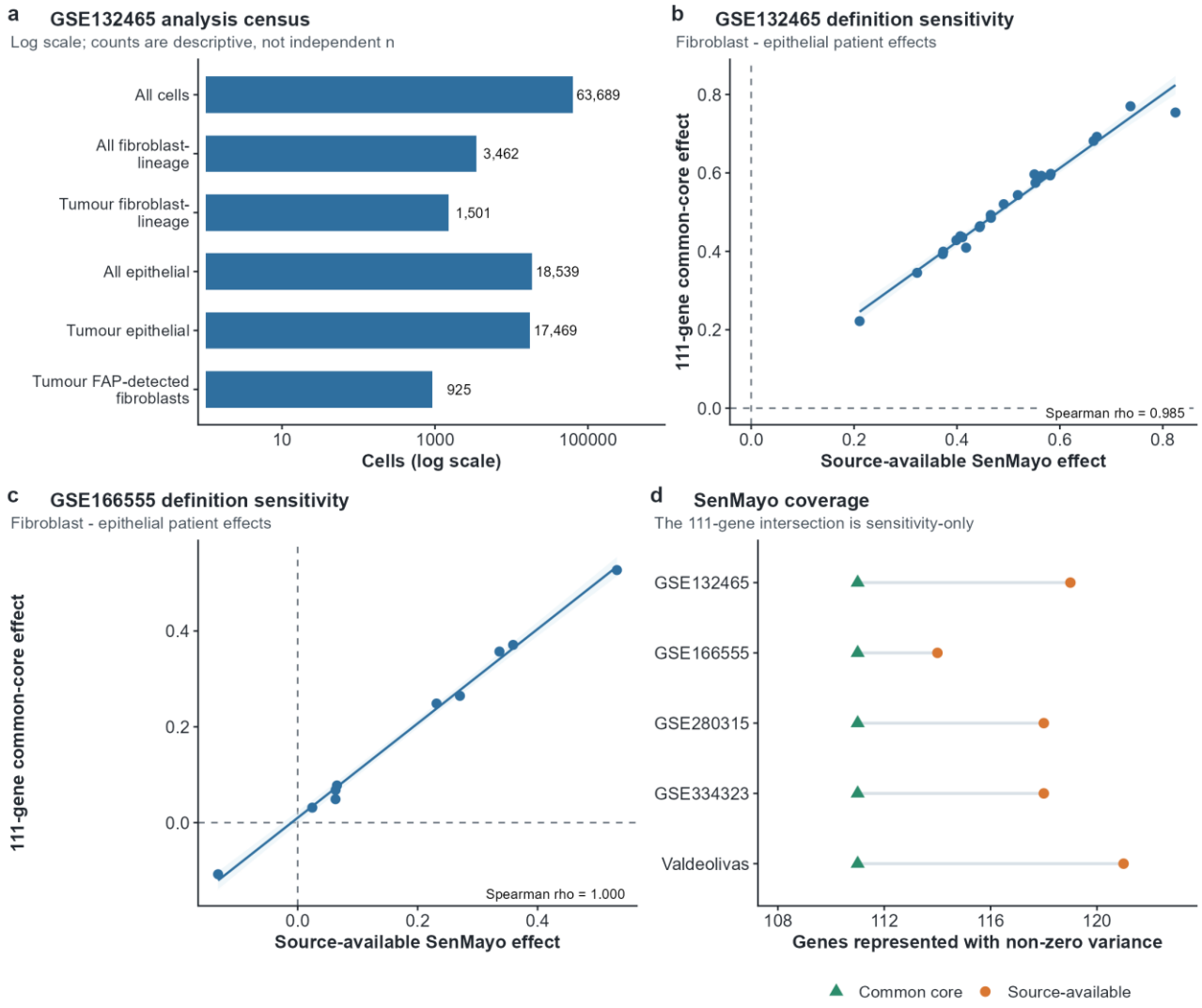
Supporting figures

Fig. S1 Dataset flow, eligibility and evidence hierarchy



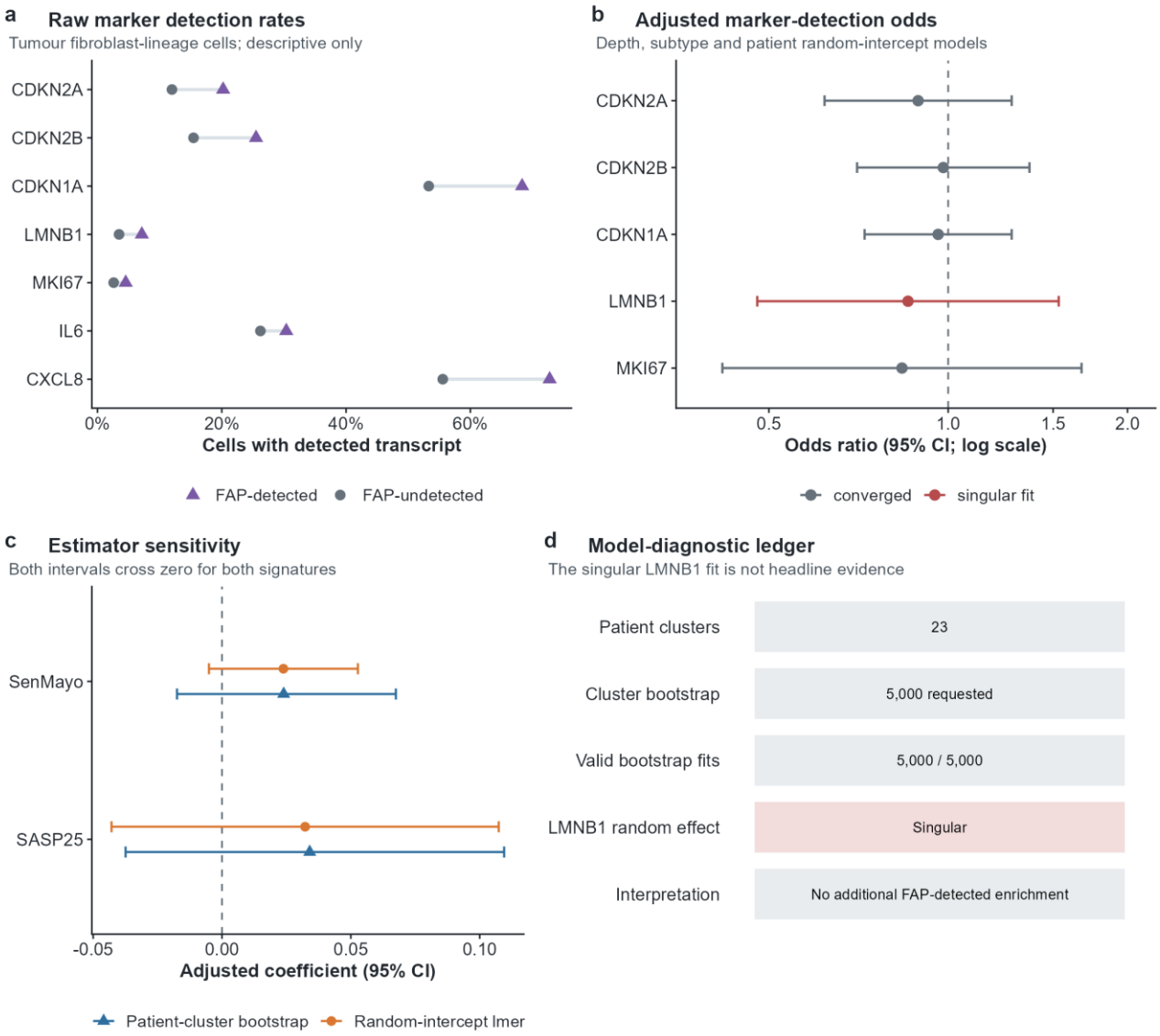
(a) Evidence architecture from paired single-cell localization through within-fibroblast boundary analyses, bulk and protein triangulation, and the spatial generalizability stress test. (b) GSE132465 filtering and tumour fibroblast subgroup counts; cell counts are descriptive and the patient remains the inferential unit. (c) SenMayo overlap control: four FAP13-overlapping genes were removed from the 125-gene source list, yielding 121 candidates, 119 represented genes in GSE132465, 114 represented genes in GSE166555 and an exact 111-gene cross-dataset common core. (d) Interpretation ceiling separating measured compartment contrasts and molecular covariation from unmeasured stable arrest, cell-to-cell transfer and causality.

Fig. S2 Cell census and SenMayo definition sensitivity



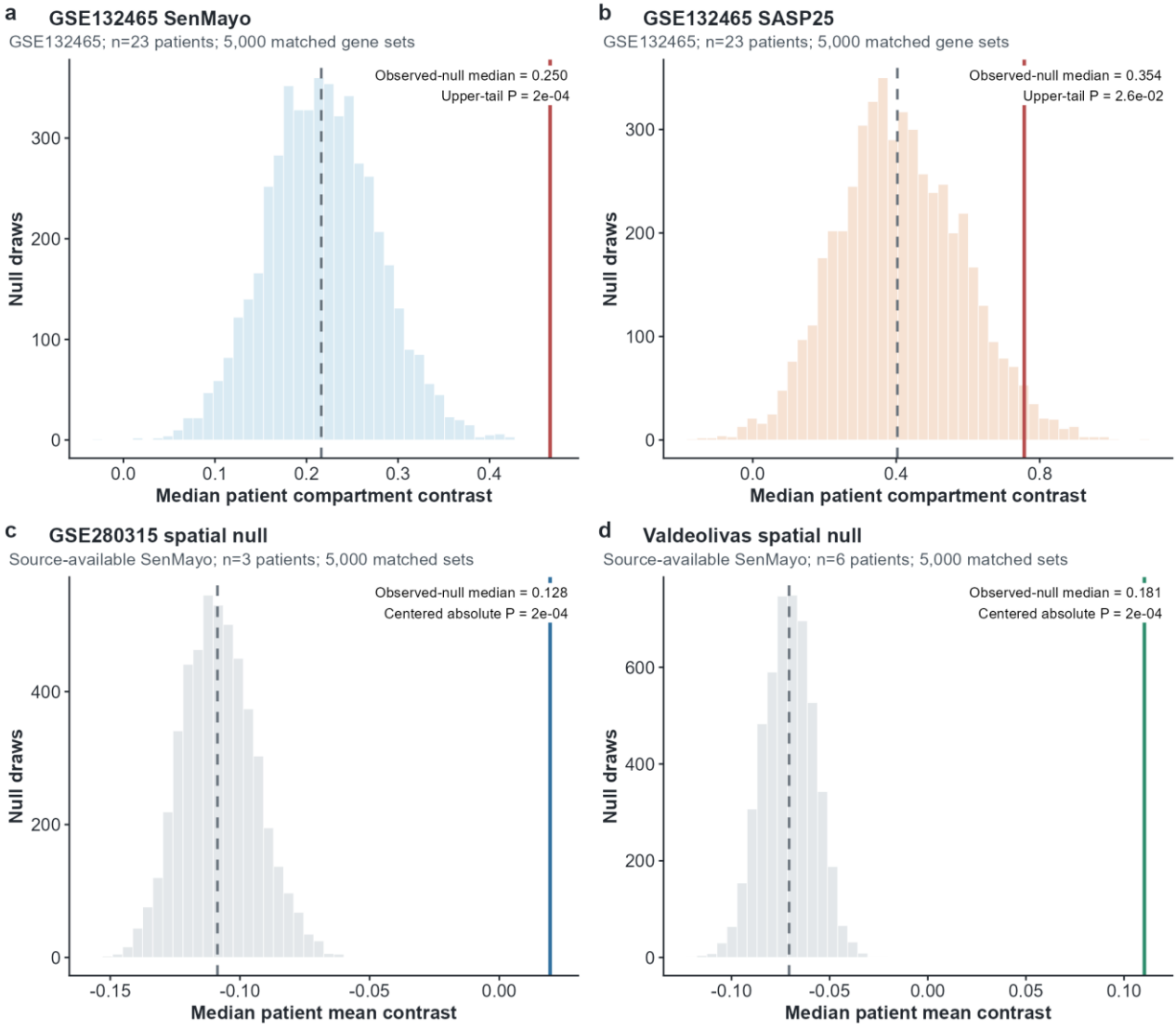
(a) GSE132465 cell census on a logarithmic scale; counts do not increase the biological sample size. (b,c) Association between patient-level source-available and 111-gene common-core fibroblast-minus-epithelial effects in GSE132465 and GSE166555, respectively. (d) Source-available and common-core gene representation across both single-cell and all three spatial cohorts. The common core is used only as a sensitivity analysis.

Fig. S3 Single-gene boundary analyses and model diagnostics



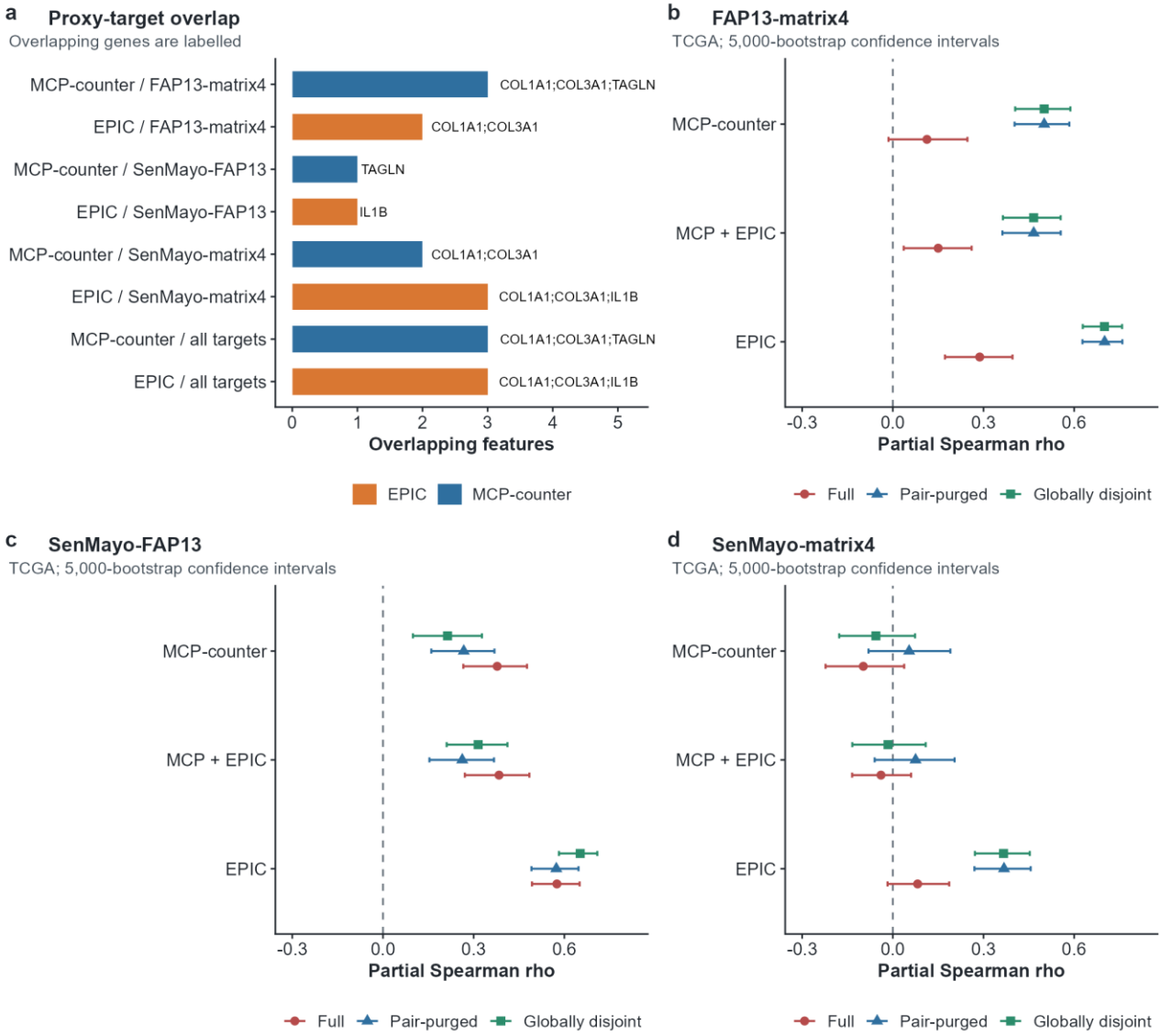
(a) Descriptive transcript-detection rates for selected arrest, proliferation and SASP-related genes in FAP-detected and FAP-undetected GSE132465 tumour fibroblast-lineage cells. (b) Adjusted odds ratios for detection of CDKN2A, CDKN2B, CDKN1A, LMNB1 and MKI67 from depth-, subtype- and patient-adjusted random-intercept models. The LMNB1 model was singular and is retained as a diagnostic rather than headline evidence. (c) Comparison of conventional random-intercept and patient-cluster-bootstrap estimates for FAP-detected SenMayo and SASP25 coefficients; confidence intervals cross zero. (d) Model-diagnostic ledger, including the number of patient clusters and successful bootstrap fits. These analyses do not establish equivalence between FAP-detected and FAP-undetected cells.

Fig. S4 Expression-matched null diagnostics



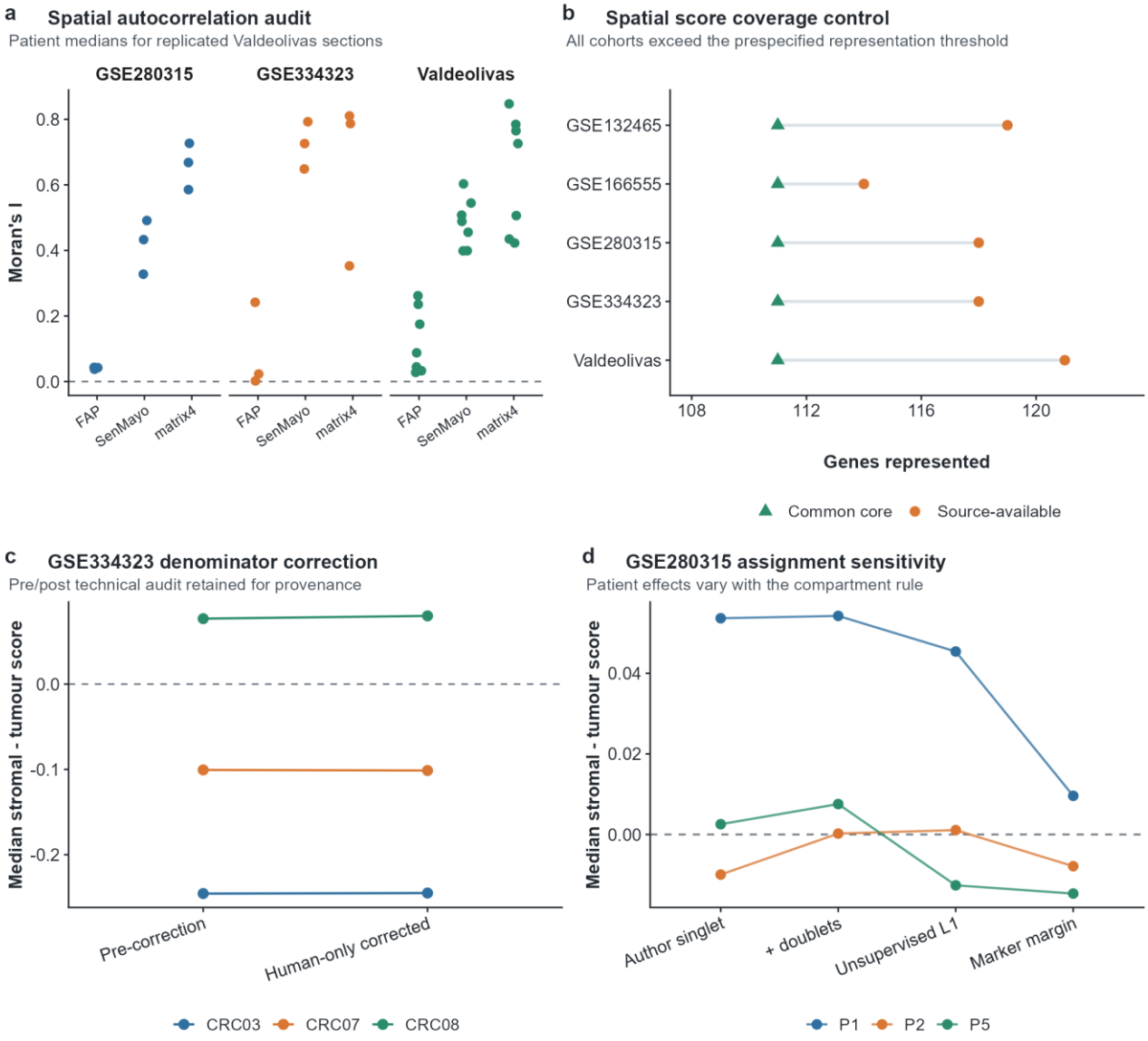
(a,b) GSE132465 distributions of 5,000 expression-, variability- and detection-matched gene-set statistics for the median patient fibroblast-minus-epithelial contrast, shown for SenMayo119 and SASP25. Solid coloured lines mark the observed statistics and dashed grey lines the null medians. (c,d) Corrected centered matched-null analyses for the source-available SenMayo definitions in GSE280315 and the Valdeolivas cohort. The displayed spatial empirical P values compare the absolute observed displacement from the null centre with the centered null distribution. Biological sample sizes and Monte Carlo draw counts are labelled separately.

Fig. S5 Composition-proxy overlap and target-purge sensitivity



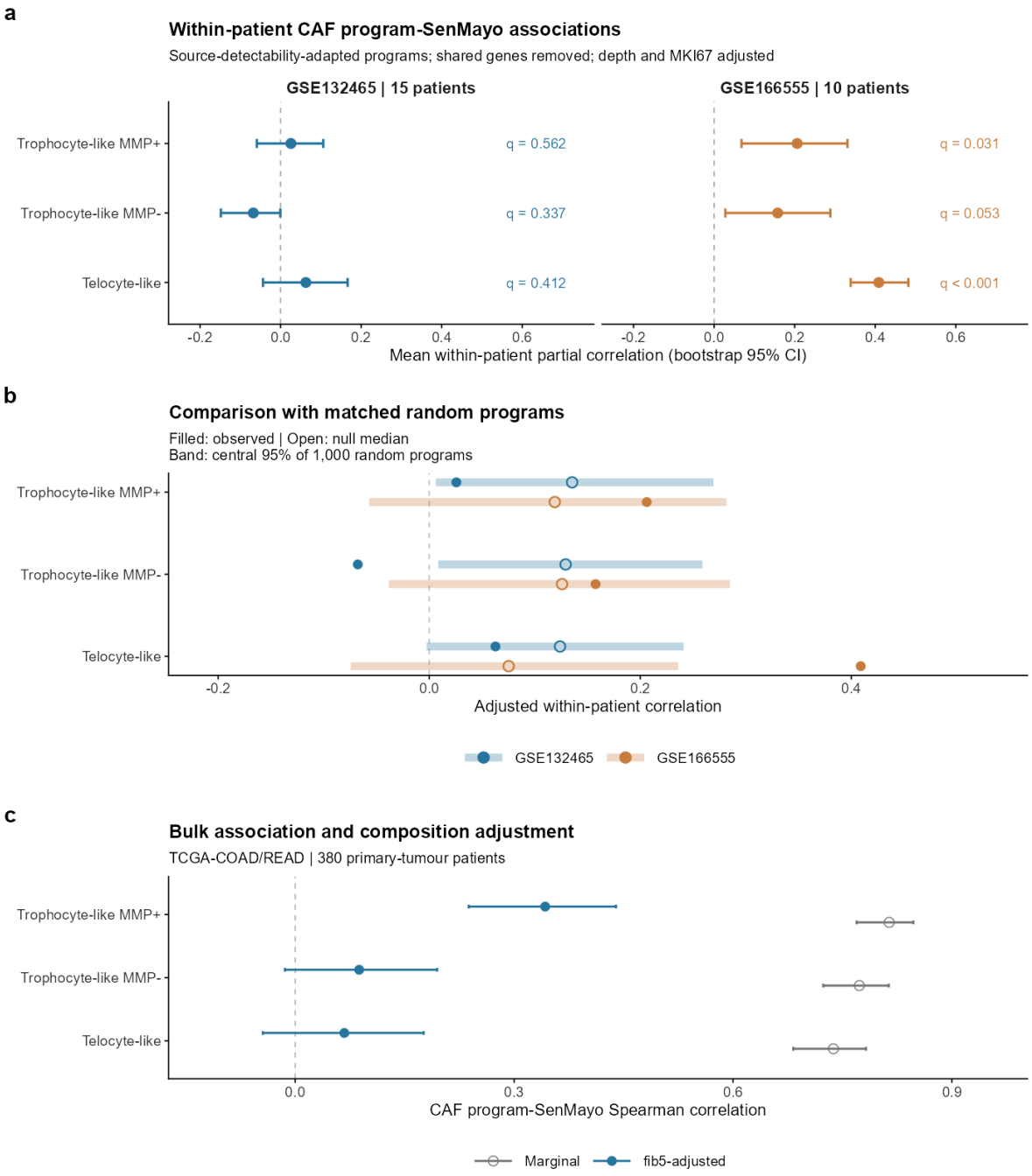
(a) Numbers and identities of target genes incorporated into the frozen MCP-counter and EPIC fibroblast/CAF proxy features. (b–d) TCGA partial Spearman correlations for FAP13–matrix4, SenMayo–FAP13 and SenMayo–matrix4 under full, pair-purged and globally disjoint MCP-counter, EPIC and joint proxy definitions. Confidence intervals were obtained from 5,000 patient bootstrap resamples. Changes across definitions are interpreted as composition-proxy sensitivity, not as proof that an association is composition driven or composition independent.

Fig. S6 Spatial quality control and provenance



(a) Patient-level or patient-aggregated Moran's I values for FAP, matrix4 and SenMayo across GSE280315, GSE334323 and the Valdeolivas cohort. (b) Spatial-cohort source-available and 111-gene common-core coverage. (c) GSE334323 stromal-minus-tumour effects before and after removal of 323 microbial, viral or control features from the library-size denominator; both versions are retained for provenance. (d) GSE280315 patient effects under author singlet, singlet-plus-doublet, author unsupervised and frozen marker-margin compartment definitions. The panel documents sensitivity to the compartment-assignment rule.

Fig. S7 CAF marker programmes and senescence-associated transcription



(a) Mean patient partial correlations with 95% patient-bootstrap intervals after library-size and MKI67 adjustment; q values are from cohort-specific Benjamini–Hochberg-adjusted t tests. (b) Filled points show observed correlations, open points show random-programme medians and bands show central 95% reference ranges, not confidence intervals. (c) TCGA programme–SenMayo correlations before and after fib5 adjustment, with 95% bootstrap intervals. MMP, matrix metalloproteinase. All programmes are source-detectability-adapted scores, not subtype assignments. Details and limitations are given in the supporting methods.

Supporting methods for the exploratory CAF analysis

Source provenance and detectability adaptation

Marker statistics were taken from Supplementary Table 5 (sheet “Table 5 scRNA cell type markers”) of Buissant des Amorie et al., Nature 2026;654:229–239 (doi: 10.1038/s41586-026-10344-7). The source early-stage tumour-microenvironment experiment included 222 fibroblasts from five patients. The article separately integrated GSE132465 into a larger public atlas; the Table 5 marker experiment was not that integrated atlas. Thus, the marker source and our GSE132465 analysis are distinct experiments, but independence from every analysis in the source publication is not claimed. GSE166555 was an external cohort, not a bulk validation cohort. Source CAF–organoid experiments are cited as published functional context and were not reproduced in this study.

The initial extraction selected up to 100 positive markers per source cluster with adjusted $P < 0.05$, ordered by descending average log2 fold change and then alphabetically to break ties. Only 15, 9 and 18 genes, respectively, were represented across both single-cell matrices; overlap removal reduced these to 12, 9 and 18. None met the prespecified 50-gene evaluability threshold, so no target-association result was generated from this extraction. Before new target-association testing, source detection was added as an eligibility requirement: $pct.1 \geq 0.25$ and $pct.1 - pct.2 \geq 0.10$, with the same adjusted-P and fold-change requirements and top-100 ranking. This adaptation used source statistics, not the direction or significance of correlations in the target cohorts. Exposure genes overlapping the full 125-gene SenMayo list, FAP13, matrix4, fib5 or MKI67 were removed without backfilling. The resulting MMP-positive trophocyte-like, MMP-negative trophocyte-like and telocyte-like programmes contained 84, 88 and 90 genes before target-platform intersection, and 82, 86 and 85 genes in the shared single-cell universe. Unadapted and adapted memberships, source ranks and all exclusions are retained in S1 Data.

Cell selection and scoring

In GSE132465, applying the ≥20-fibroblast threshold to the 1,501 tumour fibroblast-lineage cells used in the main analysis retained 1,435 cells from 15 patients; eight patients contributing 66 cells were excluded by cell count, not outcome. GSE166555 contributed 1,315 tumour fibroblasts from the ten patients already eligible for the main paired-compartment analysis, using the original fibroblast/CAF/myofibroblast annotations. Library sizes were checked against the retained cell metadata. For GSE132465, retaining genes detected in at least three cells across the complete 63,689-cell source dataset recovered the archived 25,655-gene normalization universe and exact library sizes. GSE166555 used its 21,854-gene public matrix and also matched the retained library sizes. Counts were transformed as $\log1p(10{,}000 \times \text{count/library size})$. Genes were standardized across eligible fibroblasts within each cohort, and programme scores were arithmetic means of gene-wise z scores. Zero-variance genes contributed zero. Of the 114 shared SenMayo genes, 113 and 107 were non-constant in these GSE132465 and GSE166555 fibroblast populations, respectively. The outcome was defined in

this within-fibroblast universe and did not replace the source-available compartment scores or the 111-gene cross-platform sensitivity reported in the main analyses.

Patient-level association and sensitivity inference

Within each patient, programme scores, SenMayo scores, log1p library size and MKI67 expression were rank-transformed with average ranks for ties. Exposure and outcome ranks were separately residualized against an intercept and the two ranked covariates, and their residuals were correlated by Pearson correlation. Patient partial-correlation coefficients were Fisher-z transformed, averaged with equal patient weights and back-transformed with tanh. No coefficient was pooled across cohorts. The primary P value was a two-sided one-sample t test of patient Fisher z against zero, with 14 or 9 degrees of freedom. Benjamini–Hochberg adjustment covered three programmes separately within each cohort and analysis definition. Confidence intervals were 2.5th and 97.5th percentiles of 5,000 patient bootstrap estimates. Because these intervals are not inversions of the t test, interval exclusion of zero and a t-test-based P value need not coincide; multiplicity-adjusted decisions followed $q < 0.05$. T-based confidence intervals from an independent R recalculation, 50,000 patient sign-flip tests, leave-one-patient-out estimates, unadjusted models and models adding original fibroblast-subtype indicators were retained. The source-specific SenMayo definitions were also evaluated as sensitivities. Seed 2026090911 and deterministic cohort/model offsets were used for single-cell resampling.

Approximately matched random programmes

For each programme and cohort, 1,000 unique-gene sets of equal size were sampled by nearest-neighbour matching on mean log-normalized expression and transcript-detection fraction, standardized by the candidate-pool standard deviations. Candidates were non-constant genes detected in at least 1% of cells, excluding the target score genes, source CAF programme genes, MKI67 and mitochondrial/ribosomal genes. For each target gene, up to 500 nearest candidates were ranked by squared Euclidean distance; one was sampled from the first 100 unused candidates, with randomized gene order and no within-set duplicates. The same patient-level partial-correlation statistic was recomputed for each draw. The two-sided empirical P value was (1 + number of null Fisher-z means at least as far from their null median as the observed value)/1,001, with Benjamini–Hochberg adjustment across three programmes per cohort. The plotted bands are central 95% random-programme ranges, not uncertainty intervals for the observed effect. Matching was approximate: median absolute differences in set-average matching features ranged from 0.054 to 0.144 candidate-pool standard deviations. Some programmes retained systematic imbalance; these comparisons are sensitivity evidence rather than a definitive specificity test. An observed statistic below its random-programme reference was not interpreted as senescence enrichment.

Auxiliary bulk analysis and full result retention

The 380 TCGA COAD/READ primary-tumour patients from the core bulk analysis were scored with 78, 85 and 84 represented purged CAF genes, respectively. The original FAP13, matrix4,

fib5 and 119-gene bulk SenMayo scores were reproduced to a maximum absolute difference below 8×10^{-15} before adding CAF scores. Bulk SenMayo gene membership was source specific and was not equated with the 114-gene single-cell outcome. Spearman correlations and partial correlations adjusted for ranked fib5 were evaluated for every CAF programme against SenMayo, FAP13 and matrix4. Five thousand patient bootstraps supplied percentile confidence intervals; Benjamini–Hochberg adjustment covered all nine programme–target comparisons separately for marginal and adjusted models. The fib5 features were disjoint from the exposures and outcomes. They form an expression proxy, not a measured fibroblast fraction; other existing proxy definitions were not reused without a new CAF-feature overlap audit. All six primary single-cell results, six matched-null results and eighteen bulk comparisons are retained in Table S8; complete sensitivities, patient coefficients, marker coverage and random-programme diagnostics are in S1 Data. No programme met a positive $q < 0.05$ criterion in both single-cell cohorts. Different cohort-specific significance labels do not themselves demonstrate a between-cohort difference.

Supporting tables

Table S1. Dataset accessions, eligibility and checksums

File: tables/S1_Table_dataset_accessions_eligibility_and_checksums.csv

Records repository identifiers, modality, source and analysis populations, independent units, eligibility or exclusion rules, compartment-label sources, principal result artifacts and SHA-256 checksums.

Table S2. Signature membership, overlap removal and representation

File: tables/S2_Table_signature_membership_overlap_and_representation.csv

Provides one row per unique signature gene and flags membership in the source SenMayo list, overlap-purged SenMayo candidates, SASP25, FAP13, matrix4, receptor2, the 111-gene common core and each cohort's represented SenMayo set.

Table S3. Single-cell compartment statistics

File: tables/S3_Table_single_cell_compartment_statistics.csv

Reports the score definition, patient count, frozen estimand, estimate, patient-bootstrap confidence interval, direction counts and exact paired P value for source-available SenMayo, SASP25 and MKI67 in both single-cell cohorts and for the 111-gene common-core sensitivity.

Table S4. FAP-specific models and diagnostics

File: tables/S4_Table_FAP_specific_models_and_diagnostics.csv

Contains conventional mixed-model and patient-cluster-bootstrap estimates for the FAP-detected SenMayo and SASP25 models, the continuous FAP–matrix4 model, selected single-gene detection models and convergence or singular-fit diagnostics.

Table S5. Patient-level correlations and dependent contrasts

File: tables/S5_Table_dependent_patient_level_correlations.csv

Provides within-cohort Spearman correlations among FAP, SenMayo and matrix4 and the two dependent-correlation contrasts, with paired patient-bootstrap confidence intervals and sign probabilities. Correlation differences are recomputed within the same resamples.

Table S6. Bulk composition overlap and sensitivity

File: tables/S6_Table_bulk_composition_overlap_and_sensitivity.csv

Combines the TCGA and GSE39582 marginal FAP13–matrix4 correlations, TCGA partial correlations under all frozen composition-proxy definitions and the proxy-target feature-overlap audit. Estimates are reported by definition rather than collapsed into a single composition-adjusted coefficient.

Table S7. Spatial effects and provenance

File: tables/S7_Table_spatial_results_and_provenance.csv

Contains all patient or independent-section effects for source-available SenMayo, the 111-gene common core, MKI67 polarity and the FAP–matrix comparative-correlation contrast. It also records corrected spatial matched-null statistics, GSE280315 compartment-definition sensitivity and GSE334323 pre/post-denominator-correction provenance. Cohort-level tests are reported only for prespecified eligible cohorts and are not pooled across platforms.

Table S8. CAF programme associations and matched-null results

File: tables/S8_Table_CAF_programme_associations.csv

Contains all six primary single-cell estimates, six matched-null comparisons and eighteen bulk estimates. Effect confidence intervals and random-programme reference ranges are separate fields. The module column identifies the analysis family; r denotes the back-transformed mean patient coefficient in the single-cell rows, whereas rho denotes a tissue-level Spearman coefficient in the bulk rows.

Companion source-data files

- tables/S2_Data_SenMayo_cohort_coverage_summary.csv: cohort-specific source-available and common-core gene counts.
- tables/S3_Data_patient_compartment_scores.csv: patient-compartment SenMayo, SASP25 and MKI67 values underlying Fig. 1 and Table S3.
- tables/S3_Data_common_core_patient_effects.csv: patient-level common-core effects underlying Fig. S2 and Table S3.
- tables/S7_Data_spatial_primary_tests.csv: archived cohort-level H1/H2 signed-rank tests and Holm adjustments for the two prespecified test cohorts.

S1 Data. CAF source-data archive

File: S1_Data_CAF_programme_source_data.zip

Contains source and adapted marker lists, gene coverage, frozen patient and cell scores, complete association and sensitivity tables, matched-programme distributions and diagnostics, figure source tables and a SHA-256 manifest. This source-data archive accompanies the exploratory analysis and is also included in GitHub release v2.1.1.